Dynamics of Nano-Meter-Sized Domains on a Vesicle

Y. Sakuma, N. Urakami[*], Y. Ogata[*], M. Nagao[†¶], S. Komura[§], and M. Imai

Department of Physics, Ochanomizu University, Bunkyo, Tokyo112-8610, Japan
[*]*Department of Physics and Information Sciences, Yamaguchi University, Yoshida, Yamaguchi 753-8512, Japan*
[†]*Cyclotron Facility, Indiana University, Bloomington, IN 47408-1398, USA*
[¶]*Center for Neutron Research, National Institute of Standards and Technology, Gaithersburg, MD 20899-6102, USA*
[§]*Department of Chemistry, Tokyo Metropolitan University, Minami Osawa, Tokyo 192-0397, Japan*

Abstract. We have investigated the dynamics of nano-meter-sized domains on a vesicle composed of saturated phospholipids, unsaturated phospholipids and cholesterols by means of a neutron spin echo technique. The diffusion coeffisient of the domains obtained from the intermediate scattering function is about two orders of magnitude larger than that calculated by Saffman and Delbrück law. From molecular dynamics simulations we found another type of the domain dynamics where the domains are agitated by thermal fluctuation and repeats coalescence and rupture. The relaxation rate of the new mode is about two orders of magnitude larger than that of the diffusion mode. The coalescence and rupture mode of domains may be responsible for the observed domain dynamics.

Keywords: Domain dynamics, Lipid raft, Nano-meter-sized domain, Neutron spin echo, Small unilamellar vesicle
PACS: 87.14.Cc, 87.14.dt, 87.16.dr

INTRODUCTION

In cell membranes, the constituents form characteristic lateral heterogeneities arising from the immiscibility of the lipid components such as sphingomyelin, unsaturated phospholipids, and cholesterol (Chol). The heterogeneitis coupled with the specific protein distribution are responsible for the important biological functionalities such as endocytosis, adhesion, signaling, protein transport and apoptosis and called lipid rafts [1,2]. Due to the wealth of biological significance of the lipid raft model, the structure of lipid rafts in cell membranes has been investigated using many techniques, which have shown that the size of lipid raft is nano-meter length scale. On the other hand, the dynamical nature of the raft is still controversial [3-5]. One of the important points of the raft is whether the raft is stable entity in the cell membranes or dynamically fluctuating platform, which is closely related to the mechanism of the biological functionalities.

In order to understand the statical and dynamical nature of the lipid raft, the model biomembrane systems consisting of phospholipids and cholesterol have also been investigated [6-8]. For example, it has been shown that the model vesicles composed of saturated phospholipids, unsaturated phospholipids and cholesterols exhibit lateral phase separation between L_o (liquid-ordered) phase and L_d (liquid-disordered) phase below a miscibility temperature T_m, which is observed as micro-meter-sized liquid domain structure by a fluorescence microscopy. The diffusion of micro-meter-sized domains on a giant vesicle was visited by Keller and our groups. The former group showed that the diffusion of domains follows the Saffman and Delbrück law [9]

$$D(r) = \frac{k_B T}{4\pi\eta\delta}\left[\ln\left(\frac{\eta\delta}{\eta_w r}\right) - \gamma\right] \qquad (1)$$

where D is the diffusion coefficient, η and η_w are the viscosities of the membrane and water, respectively, δ is the membrane thickness, γ=0.5772 and r is the radius of domain [10], whereas we claimed that the hydrodynamic flow in the membrane affects the diffusion of domains [11]. The behavior of the micro-meter-sized liquid domains on the model biomembranes is well understood by the direct observations, while that of the nano-meter-length scale

CP982, *Complex Systems, 5th International Workshop on Complex Systems*
edited by M. Tokuyama, I. Oppenheim, and H. Nishiyama

domains is poorly understood due to the optical resolution limit of the microscopy.

In this study we prepare small unilamellar vesicles (SUVs) with nano-meter length scale for spatial confinement, which makes it possible to focus our attention on the nano-meter-sized domains. In order to reveal the dynamical structure we adopt the small angle neutron scattering (SANS) and the neutron spin echo (NSE) techniques. A unique feature of the neutron scattering is that a hydrogen atom and a deuterium atom have different scattering lengths. We prepare SUVs using deuterated saturated lipid, protonated unsaturated lipid and protonated cholesterol and obtain the information on the deutrated domains in the SUV. In addition we perform molecular dynamics simulations with a coarse grained model to reproduce the phase separation on a SUV. By comparing the SANS, NSE and the simulation results we elucidate the statical and dynamical nature of nano-meter-sized domains in the SUV.

EXPERIMENTS

Commercial Reagents

1,2-dioleoyl-sn-glycero-3-phosphocholine (DOPC) (> 99 % purity), 1,2-dipalmitoyl-sn-glycero-3-phosphocholine (*h*-DPPC) (> 99 % purity) and 1,2-dipalmitoyl-d62-sn-glycero-3-phosphocholine (*d*-DPPC) (> 99 % purity) were obtained in a powder form from Avanti Polar Lipid, Inc. (Birmingham, AL) [12]. Cholesterol (Chol) (> 99 % purity) was purchased from Sigma-Aldrich Co. (St. Louis, MO) [12]. In this study we fixed the vesicle composition of *d*-DPPC/DOPC/cholesterol = 4/4/2 (mole ratio) having T_m = 29°C, because it shows a nucleation-growth type phase separation in observed temperature region.

Sample Preparation

We prepared SUVs by the following procedure. First we dissolved the lipids (DPPC, DOPC and Chol) in chloroform (5mM) and then the solutions were mixed at the prescribed ratio of DOPC, DPPC and Chol in a vial. The chloroform was evaporated in a stream of nitrogen gas and then the obtained lipid film was kept under vacuum for one night to remove the remaining organic solvent completely. The dried lipid film was dispersed in 1 ml of pure water at 60 °C, which results in the formation of micro-meter-sized vesicles (giant vesicles). The suspension of vesicles with milky appearance was sonicated using a ultrasonic homogenizer with 20kHz frequency (Yamato, Powersonic Model 50 [12]) for 30 min. After the sonication we obtained SUVs with radius of ≈100Å and the suspension became transparent.

Small Angle Neutron Scattering Measurements

In this study we performed SANS experiments under two experimental conditions, one is a film contrast condition where we can obtain whole shape of the SUVs and the other is a contrast matching condition where we can estimate the lateral heterogeneity in the SUVs. In the film contrast condition, we used *h*-DPPC/DOPC/Chol ternary vesicles in D_2O solvent, whereas in the contrast matching experiment, we substituted *d*-DPPC for *h*-DPPC to extract the domain structure on the vesicle. At this matching condition (the H_2O volume fraction of the matching solvent; ϕ^*_{H2O}=0.548) we observed no scattering from SUVs in the homogeneous one-phase region. Decreasing temperature from the one-phase region to two-phase region, the lateral phase separation takes place at the miscibility temperature, where *d*-DPPC rich L_o phase coexists with DOPC rich L_d phase. Then the scattering length densities (SLDs) of the domain ρ_d and the matrix ρ_m do not match with SLD of the solvent ρ_{solv}. These SLD differences bring a characteristic scattering function.

The SANS measurements were performed using the SANS-U instrument of the Institute for Solid State Physics, The University of Tokyo at JRR-3M of the Japan Atomic Energy Agency [13,14].

Neutron Spin Echo Experiments

In order to reveal the dynamics of nano-meter-sized domains we performed NSE experiments under two experimental conditions, one is the film contrast condition where we can obtain the dynamics of whole shape of the SUVs and the other is the contrast matching condition where we can estimate the dynamics of nano-meter-sized heterogeneity in the SUVs.

The NSE experiments were performed using NG5-NSE spectrometer at the NIST Center for Neutron Research [15,16]. Incident neutron wavelength of 6 Å was selected by a mechanical neutron velocity selector with a wavelength resolution of about 20 %. The measured momentum transfer, q, covered the range (0.047 to 0.09) $Å^{-1}$ and the time range was (0.05 to 15) ns. The DAVE software package was used for elements of the data reduction and analysis [17].

RESULTS AND DISCUSSIONS

Domain Formation on SUVs

First, we checked the shape and the size of the SUVs. We obtained the SANS profiles from SUVs at the film contrast condition at 333.2 K (homogeneous phase) which is well described by the model scattering function for the spherical shell structure. From the fitting we extracted mean outer radius of vesicles R_{out} = (112±11) Å, the bilayer thickness δ = (42±6) Å and the size polydispersity ($p^2 = < R_{in}^2 > / < R_{in} >^2 - 1$) p= (0.32±0.02), and these values were independent of the temperature.

Next, we investigated the nano-meter-sized domain formation on the SUVs with $R \approx 110$Å using the contrast matching technique of SANS experiments. The SANS profiles of the SUV are shown in Fig. 1. At 333.2K where the SUVs are in one phase homogeneous region, we observed no significant scattering from the vesicles, indicating that the DOPC, Chol and DPPC are mixed molecular level and each SUV has almost uniform composition. When we decreased temperature to the phase separation region (285.2 K), excess scattering intensity due to the domain formation was observed as shown in Fig. 1. The scattering intensity profile has a maximum in the vicinity of q = 0.03 Å^{-1}, which is a characteristic scattering pattern from domains on a vesicle at the matching condition and the peak position depends on the vesicle size or number of domains.

Dynamics of Nano-meter-sized Domains

In order to make clear the dynamical nature of the nano-meter-sized domains, we measured the intermediate scattering function of the ternary SUVs with *d*-DPPC/DOPC/Chol = 4/4/2 at the matching condition. The intermediate scattering function is given by

$$S(q,t) = < \sum_{i,j} e^{iq\cdot[\mathbf{R}_i(t)-\mathbf{R}_j(0)]} > \quad (2)$$

where $\boldsymbol{R}_i(t)$ is the coordinates of individual lipid molecules at time t. In Fig. 2 we show the obtained intermediate scattering function for the ternary SUVs at the contrast matching condition at 285.2 K. By assuming that the intermediate scattering function consists of two components, the whole vesicle diffusion mode and the nano-meter-sized domain relaxation mode, the intermediate scattering functions were fitted by a double exponential function

$$\frac{S(q,t)}{S(q,0)} = A(q)\ \exp(-D_0 q^2 t) + (1 - A(q)) \exp(-\Gamma t) \quad (3)$$

where D_0 is the diffusion coefficient of the whole SUV, Γ is the relaxation rate of the domain relaxation mode and A is the numerical constant. The value of D_0 used here is obtained from the intermediate scattering function of the SUV at the film contrast condition.

Under the assumption that the relaxation profile of spherical vesicle is expressed by a sum of the whole vesicle diffusion mode and the vesicle deformation mode, we fitted the relaxation profile measured at the film contrast condition by a double exponential function

$$\frac{S(q,t)}{S(q,0)} = B(q)\ \exp(-D_0 q^2 t) + (1 - B(q)) \exp(-\Gamma_d t) \quad (4)$$

where Γ_d is the relaxation rate of the shape deformation mode [18]. The relaxation rate for the vesicle diffusion mode show linear relationship against q^2 and the slope gives the diffusion coefficient D_0=(1.4 ±0.01)×10^{-11} m^2/s. The diffusion coefficient can be estimated from the Stokes-Einstein equation

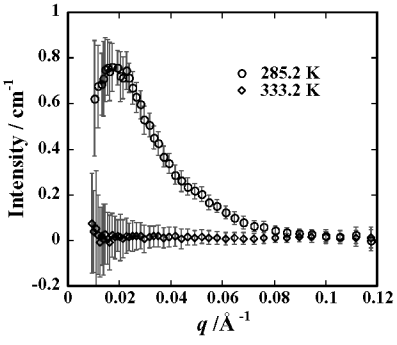

FIGURE 1. SANS profiles from SUVs at the contrast matching condition at 333.2 and 285.2 K [19]

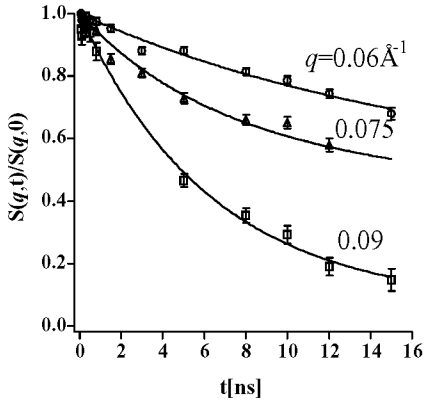

FIGURE 2. Intermediate scattering function for the ternary SUVs at the contrast matching condition at 285.2 K [19]

$$D_0 = \frac{k_B T}{6\pi\eta_w R_{out}} \qquad (5)$$

Using the values of T=285.2 K, η_w=1.3×10 Pa·s and R_{out}=112Å, the calculated D_0 is 1.6×10^{-11} m^2/s, which agrees well with the value estimated by the NSE measurement. Then the eq. (3) contains only two adjustable parameters, A and Γ, and the fitting results are shown in Fig. 2 by solid lines. The relaxation rate of the nano-meter-sized domain mode obtained from the fitting are plotted against q^2 in Fig. 3, which gives good linear relationship although we have only three points. The q dependence of Γ indicates that the vesicle deformation mode does not affect the domain relaxation mode significantly[18]. When we assume that the domain relaxation mode corresponds to the domain diffusion, the slope gives the diffusion coefficient of the domains of $(3.7\pm0.2)\times10^{-10}$ m^2/s. The Saffman and Delbrück law (eq. (1)) gives the diffusion coefficient of the domains of 2.7×10^{-12} m^2/s, which is smaller than the experimental value by about two orders of magnitude. Thus the domain diffusion model may be inadequate to explain the observed domain mode.

In order to interpret the domain dynamics on a SUV, we performed the molecular dynamics simulation. For a shallow quenched vesicle from the homogeneous state, the mono-domain is agitated by thermal fluctuations and repeats coalescence and rupture, whereas for the deep quenched vesicle, the mono-domain shows the Brownian motion on the SUV. From the time resolved simulation data in the equilibrium state we calculated the intermediate scattering function for two states. The obtained relaxation rate for the domain diffusion mode is about two orders of magnitude smaller than that of the coalescence and rupture mode. Thus the coalescence and rupture mode may correspond to the observed relaxation mode of the nano-meter-sized domains. Details of this issue will be reported in the forthcoming paper.

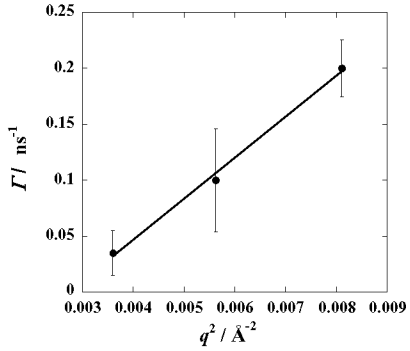

FIGURE 3. The relaxation rate of the nano-meter-sized domain mode against q^2 [19]

ACKNOWLEDGMENTS

This work utilized facilities supported in part by the National Science Foundation under Agreement No. DMR-0454672. This work was performed using SANS-U of the Institute for Solid State Physics, the University of Tokyo (Proposal No. 7606).

REFERENCES

1. K. Simons and E. Ikonen, *Nature*. **387**, 569-572 (1997).
2. M. Edidin, *Annu. Rev. Biophys. Biomol. Struct.* **32**, 257-283 (2003).
3. A. Kusumi, I. K. Honda, and K. Suzuki, *Traffic.* **5** 213-230 (2004).
4. A. Pralle, P. Keller, E. L. Florin, K. Simons. and J. K. H. Hörber, *J. Cell. Biol.* **148**, 997-1007 (2000).
5. K.Simons and W L. C. Vaz, *Annu. Rev. Biophys. Biomol. Struct.* **33**, 269-295 (2004).
6. G. W. Feigenson, *Annu. Rev. Biophys. Biomol. Struct.* **36**, 63-77 (2007).
7. S. L. Veatch and S. L. Keller, *Phys. Rev. Lett.* **89**, 268101 (2002).
8. S. L. Veatch and S. L. Keller, *Biophys. J.* **85**, 3074-3083 (2003).
9. P. G. Saffman and M. Delbrück, *Proc. Nat. Acad. Sci. USA* **72**, 3111-3113 (1975).
10. P. Cicuta, S.L. Keller and S.L. Veatch, *J. Phys. Chem. B* **111**, 3328-3331 (2007).
11. M. Yanagisawa, M. Imai, T. Masui, S. Komura and T. Ohta, *Biophysical J.* **92**, 115-125 (2007).
12. Certain commercial equipment, instruments, materials, or suppliers are identified in this paper to foster understanding. Such identification does not imply recommendation or endorsement by the National Institute of Standards and Technology, nor does it imply that the materials or equipment identified are necessarily the best available for the purpose.
13. Y. Ito, M. Imai and S. Takahashi, *Physica B* **213&214**, 889-891 (1995).
14. S. Okabe, M. Nagao, T. Karino, S. Watanabe, M. Shibayama, *J. Appl. Cryst.* **38**, 1035-1037 (2005).
15. N. Rosov, S. Rathgeber, and M. Monkenbusch, *ACS Symp. Series* **739**, 103-116 (2000).
16. M. Monkenbusch, R. Schätzler, and D. Richter, *Nuclear Instruments and Methods in Physics Research Section A* **399**, 301 (1997).
17. http://www.ncnr.nist.gov/dave
18. T. Hellweg and D. Langevin, *Physica. A* **264**, 370-387 (1999).
19. Error bars in this paper represent ± one standard deviation.